Transactions on Biomedicine and Health vol 2, © 1995 WIT Press, www.witpress.com, ISSN 1743-3525

Coupling numerical solution of bio-heat transfer equation and Maxwell's equations in biological tissues during hyperthermia

S.-C. Hwang, D. Lemmonier
Laboratoire d'Etudes Thermiques (U.R.A. CNRS 1403) E.N.S.M.A., Site du Futuroscope, B.P. 109, 86960 FUTUROSCOPE Cedex, Poitiers, France

Abstract

A coupled thermal and electromagnetic modeling of hyperthermia in biological tissues is presented. The thermal processes within the tissues are predicted by using a steady-state bio-heat transfer equation. The rate of volumetric heat generation within the tissues during the passage of microwave irradiation is obtained after solving Maxwell's field equations. All the governing equations have been solved by the finite element method, using C^0 –continuity, three-noded isoparametric elements. The numerical solutions have been validated by comparing with the analytical solutions for a simplified case. Finally, we present the temperature distributions for a real case. The effect of perfusion has been highlighted. Tumor with little blood flow rate shows good therapeutic advantage during hyperthermical irradiation.

1 Introduction

Hyperthermia--elevated tissue temperature--is a useful means for the cancer treatment, either by itself or in combination with radiation and/or chemotherapy. Many experimental and theoretical studies have confirmed the important role played by thermal processes during hyperthermia. (Mandal et al. [6]) The theoretical studies, available at present time, have been mainly based on the bio-heat transfer equation which was originally attributed to Pennes in 1948. The bio-heat transfer equation approximates a thermal energy balance in a specific tissue volume. In biological tissues, the thermal transfer is complicated by heterogeneity and the chaotic geometry of the tissue structure. The inherent limitation of the bio-heat transfer equation assumes that blood flow is non-directional at the capillary level, physically suggesting that capillaries are randomly oriented with respect to their arteriolar and venular connections. (Afuwape et al. [1])

Several approaches are possible for elevating the tissue temperature. Local heating may be produced either invasively, e.g., by small microwave antennae inserted into the tumor through hypodermic needles, or noninvasively by ultrasound transducers for superficial tumors. Regional heating has also been studied noninvasively by induction and microwave devices. Due to patient tolerance considerations, only a few thermometers can be inserted into body (typically a maximum of 4 to 5). Consequently, detailed thermal measurements are presently impractical, particularly for deep-seated tumors. The problem of temperature prediction is itself twofold : first, calculate precisely the rate of heat deposition in the various tissues by microwave irradiation, and second, predict the resultant temperature distribution. In this paper, we present numerical studies for predicting the electric and thermal field by the finite element method.

2 Mathematical model

2.1 bio-heat transfer equation

A heat balance was performed on a control volume of tissue with the following assumptions for bio-heat transfer analysis : blood flow is nondirectional at the capillary level, heat exchange between tissue and blood occurs only at this level, thermal properties within a specific tissue are isotropic, and heat generation due to microwave irradiation is included. Subject to these conditions, the bio-heat transfer equation can be written as :

$$\nabla \cdot (\lambda \nabla T) + W_b C_{pb} (T_a - T) + Q_m + Q_{wave} = 0 \qquad (1)$$

The bio-heat transfer equation expresses the energy balance between conductive heat transport in tissue $\nabla \cdot (\lambda \nabla T)$, heat loss due to perfusion effect $W_b C_{pb} (T_a - T)$, metabolism Q_m, and energy deposition specifically that due to a hyperthermia application Q_{wave}.In other words, the first term on the left hand side of equation (1) describe the heat conduction due to a temperature gradient. The second term (called pseudo-first order decay term) represents the crucial role of blood circulation in temperature regulation. W_b had been determinated using various methods such as an inverse problem where W_b is extracted from the measured temperatures. The optimal measurements of the perfusion term had been reported using Fick's dilution technique by least square minimization. (Eberhart et al. [4]). In a typical 'model' all exchanges between blood and parenchymal cells take place at the capillary level (microcirculation). True capillaries in normal tissues have a diameter close to that of an erythrocyte (7 to 10 microns) and walls consisting of three layers: endothelium, basement membrane and pericytes, and adventitia. The capillaries in tumors formed by random fusion of sprouts are tortuous, elongated, and dilated and lack basement membrane. The flow of blood through such a coarse capillary network is sluggish. A great proportion of tumor blood does not exchange with the blood in the general circulation. (called stasis phenomenon) (Perez et al [7]) For the

sake of simplicity, we assume that W_b is zero in the region of tumor. We solve equation (1) with the natural convective boundary condition.

2.2 Maxwell's equations

Electromagnetic (EM) field interacts with tissue in three basic ways : (1) orientation of electric dipoles that already exist in the atoms and molecules in the tissue, (2) polarization of atoms and molecules to produce dipoles moments, (3) displacement (or drift) of conduction ('free') electrons and ions in the tissue. Heat can be generated in the tissue in each of these three interactions. In orientation and polarization, the 'friction' associated with the movement of the atoms and molecules causes heat to be generated when a time varying EM field is applied. In the displacement of conduction electrons, the collisions of the electrons with the immobile atoms and molecules of the tissue structure produce heat. Noteworthy, it is only the internal electric field that transfers the energy to the tissue that is manifested as heat. The internal magnetic field imports no net energy to the tissue, however an incident magnetic field can produce an electric field in the tissue and that induced electric field does generate heat. (Christensen et al. [3])

The Maxwell's equations which govern the variation of the electric and magnetic field vectors $\vec{E}_c(x,y,z)$ and $\vec{H}_c(x,y,z)$ in complex form within isotropic tissues under the condition of no accumulation of static charges are given as :

$$\nabla \times \vec{H}_c - (\sigma - \omega\gamma i)\vec{E}_c = 0 \qquad (2)$$

$$\nabla \cdot \vec{E}_c = 0 \qquad (3)$$

$$\nabla \times \vec{E}_c - \omega\mu \, i \, \vec{H}_c = 0 \qquad (4)$$

$$\nabla \cdot \vec{H}_c = 0 \qquad (5)$$

Taking curl of the equation (2) and (4), one obtains :

$$\nabla^2 \vec{E}_c + \kappa^2 \vec{E}_c = 0 \qquad (6)$$

$$\nabla^2 \vec{H}_c + \kappa^2 \vec{H}_c = 0 \qquad (7)$$

with $\kappa^2 = \omega^2 \mu\gamma + \omega\mu\sigma$

We then solve the Helmholtz equation (6) with the Dirichlet type prescribed E_z boundary condition for the special case where $\vec{E}_c = E_z \hat{e}_z$. Since the electromagnetic irradiation is of very high frequency. The volumetric rate of heat generation averaged over time is given by:

$$Q_{wave} = \frac{\sigma}{2}\vec{E}_c \cdot \vec{E}_c^{*} = \frac{\sigma}{2}E_z E_z^{*} \qquad (8)$$

3. Results

3.1 Test case 1 (muscle + fat : $0 \leq r \leq 22$ cm - muscle; $22 \leq r \leq 24$cm - fat)
It is easy to find the analytical solution $E_z(r)$ for an heterogeneous cylinder. **Figure 1** shows the excellent agreements between the obtained numerical solutions and the founded analytical solutions. At the interface between muscle and fat , there is a discontinuity for Q_{wave} for reasons of the abrupt change of magnetical permittivity and electrical conductivity. Muscle absorbs more energy (exactly 0.6/0.2=3 times) than fat at interface, see table 1a.

3.2 Test case 2 (tumor+muscle+fat : $0 \leq r \leq 6$cm - tumor : $22 \leq r \leq 24$ cm - fat)
We assume a tumor embedded deeply at center, which size is equal to $(6 \times 6 \times \pi)\,cm^2$. Applying one/two/three microwave sources (0-120-240° apart) to the cylinder, we have obtained the following numerical results. In the case of only one microwave source, the maximum temperature (42.9°c) is near to the interface between muscle and fat. Similarly, in the two microwave sources case , the highest temperatures (42.9-43°c) are still near to the interface, but there is a local maximum (41.4°c) at the center of the tumor. Finally, for the three microwave sources case, the maximum temperature is 45.9°c at the center of the cylinder.(see **figure 2**), and there are three local maxima (43.1-43.2°c) near to the interface!

3.3 real case
To illustrate the ultimate use of our algorithms, we present a realistic problem based on CT scan data. **Figure 3** displays a thoracic cross section containing a tumor mass embedded deeply in the left lung and the finite element discretization for the thorax itself. We have solved this problem by modifying some temperature boundary conditions (simulation of the cooling effect in the bolus), because with all the natural convective boundary conditions, one takes a risk of overheating superficial tissues excessively. In order to focus heating in the tumor region, we have partially introduced the Dirichlet type boundary condition (prescribed temperature = T_{amb}) within the passage of three microwave irradiations. With this modification, the highest temperature (52.5°c) is in the region of the tumor. (see **figure 3**). The tumor blood perfusion rate plays a significant role in shaping the thermal profiles. We show the effects on the thermal distributions caused by raising blood flow rates in the malignant tissue. For the case where the tumor is necrotic i.e. blood flow rate null, a satisfactory temperature distribution profile in the tumor zone.(**figure. 4.a**) Increasing slightly the tumor blood flow rate to $0.066\,Kg/m^3 \cdot s$(15.2% of flow rate of muscle) has only minor effect on the temperature distribution(**figure 4.b**). When the tumor blood flow vary between $0.3 \sim 0.433\ Kg/m^3 \cdot s$, the thermal profiles change slightly, and we still have the fair temperature

distributions(**figures 4.c and 4.d**). But for the high tumor blood flows (6.98 ~ 69.8 $Kg/m^3 \cdot s$), the thermal profiles degenerate completely, and we have a very poor heating of the tumor(**figure 4.e and 4.f**). In general, we have observed that if the tumor has a blood perfusion rate significantly less than the surrounding normal tissue (specifically the muscle and fat layers), then fair thermal distributions were obtainable. On the other hand , if the tumor blood flow was on the order of or higher than those in the muscle and fat regions, little or no therapeutic heating is possible.

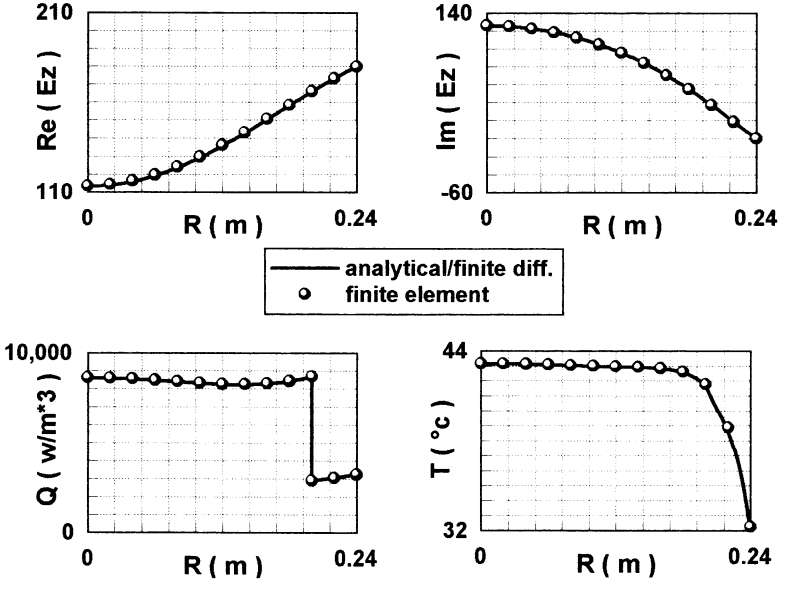

Figure 1 Comparison of solutions for a heterogeneous cylindrical testing case at 13 MHz.(analytical/finite diff. vs. finite element)

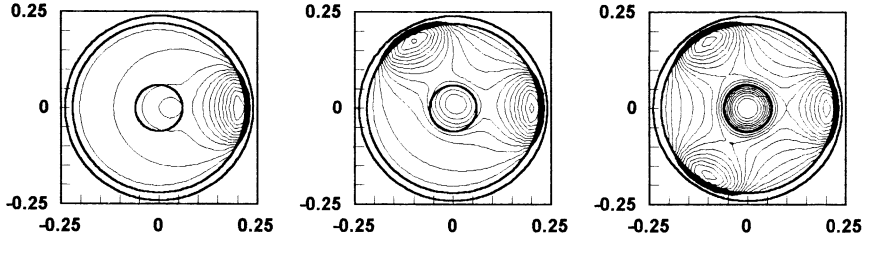

Figure 2 Application of 1/2/3 microwaves to the cylindrical testing case at 13 MHz. $(37 \leq T \leq 45\ ^\circ C\ ;\ \Delta T = 0.5\ ^\circ C)$

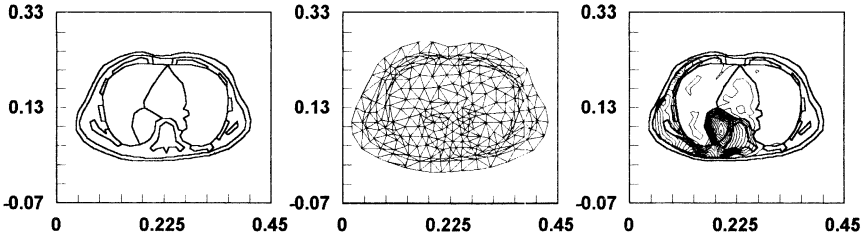

Figure 3 Geometry of the thoracic section, finite element discretisation, and temperature distribution contours.

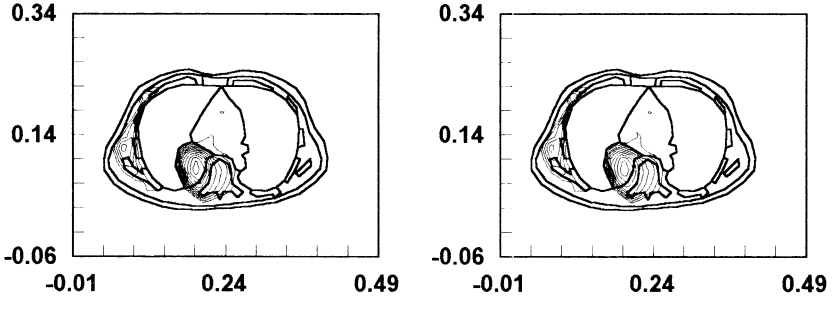

(a) (b)

Figure 4 : Isothermal lines for tumor $(38 \leq T \leq 43°C\ ;\ \Delta T = 0.5\ °C)$
a) $W_b = 0\ Kg/m^3 \cdot s$ - (b) $W_b = 066\ Kg/m^3 \cdot s$

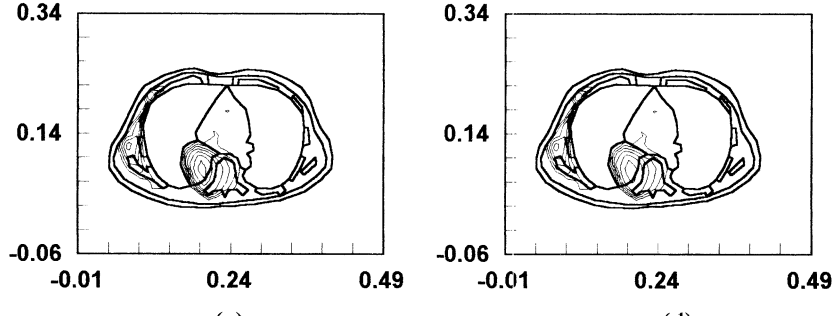

(c) (d)

Figure 5 : Isothermal lines for tumor $(38 \leq T \leq 43°C\ ;\ \Delta T = 0.5\ °C)$
c) $W_b = 0.3\ Kg/m^3 \cdot s$ - (d) $W_b = 433\ Kg/m^3 \cdot s$

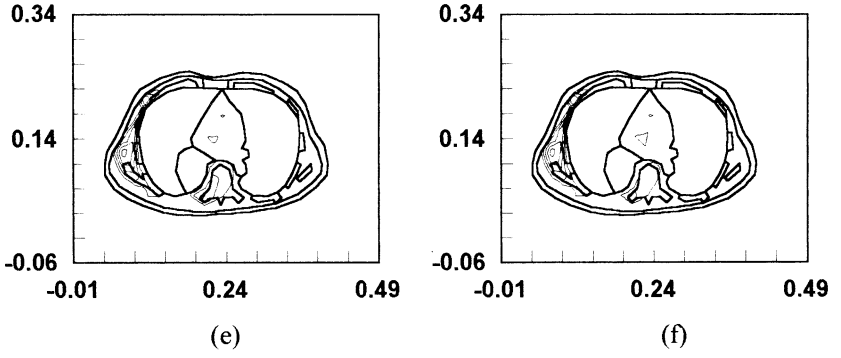

Figure 6 : Isothermal lines for tumor $(38 \leq T \leq 43°C\ ;\ \Delta T = 0.5\ °C)$
e) W_b =6.98 Kg / $m^3 \cdot s$ - (f) W_b =69.8 Kg / $m^3 \cdot s$

4 Conclusion

In this present work, the temperature distribution during hyperthermia had been predicted based only on the thermal and electromagnetic properties of the tissue, the perfusion rate of blood, and the characteristics of the incident irradiations. The blood perfusion is the critical parameter in the bio-heat transfer process, which is most difficult to quantify prior to a treatment. Based on the comparisons with the analytical/finite difference solutions, we are confident that our finite element algorithms effectively solve Maxwell's equations and bio-heat transfer equation.

Table 1a Electromagnetic properties for different tissues at various frequencies.(Lynch et al.[5])

		13 MHz	40 MHz	70 MHz	100 MHz
muscle	γ/γ_0	122.0	97.30	85.00	72.00
	σ	*0.600*	*0.693*	*0.802*	*0.889*
lung	γ/γ_0	3.200	30.00	40.00	40.00
	σ	*0.007*	*0.150*	*0.350*	*0.350*
fat	γ/γ_0	28.00	14.60	10.50	10.50
	σ	*0.200*	*0.200*	*0.210*	*0.220*
heart	γ/γ_0	140.0	70.00	89.00	0.890
	σ	*0.600*	*0.760*	*0.930*	*0.930*
bone	γ/γ_0	28.00	7.860	10.00	10.00
	σ	*0.200*	*0.020*	*0.020*	*0.020*

$\gamma_0 = 8.854 \times 10^{-12}$ F / m
$\mu = \mu_0 = 4\pi \times 10^{-7}$ H / m

Table 1b Physical and thermophysical properties of organ.(Chen et al.[2])

	$\lambda(W/m\cdot^{\circ}K)$	$W_b(Kg/m^3\cdot s)$	$Q_m(W/m^3)$
fat	0.200	0.300	269.00
muscle	0.545	0.433	703.50
bone	1.160	0.066	115.50
heart	0.586	13.55	34980.
lung	0.487	69.80	15075.
tumor	0.640	0.000	0.0000

References :

1. Afuwape S.A. & Bruley D.F. Coupling of EM microwave energy deposition with distributed perfusion for therapeutic thermal distribution, *ASME winter annual meeting,* 1989, **HTD-Vol. 126**, 67-74.

2. Chen Z.P., Miller W.H., Roemer R.B., & Cetas T.C. Errors between two- and three dimensional thermal model predictions of hyperthermia treatments, *Int. J. Hyperthermia*, 1990, **6**(1), 175-191.

3. Christensen D.A., & Durney C.H. Hyperthermia production for cancer therapy : a review of fundamentals and method, *Journal of Microwave Power*, 1981, **16** (2), 89-105.

4. Eberhart R.C.,Shitzer A.S., and Hernandex E.J. Thermal dilution methods : estimation of tissue blood flow and metabolism., *Annals of the New York academy of sciences,* 1980, **335**, 107-132.

5. Lynch D.R., Paulsen K.D., & Strohbehn J. W. finite element solution of Maxwell's equations for hyperthermia treatment planning, *Journal of Computational Physics* 1985, **58**, 246-269.

6. Mandal S., Sundararajan T., & Ghoshdastidar P.S.,1989, A coupled analysis of thermal and electromagnetic phenomena during hyperthermia in biological tissues. *ASME winter annual meeting,* 1989, HTD-Vol. **126,** 59-66.

7. Perez C.A. and Brady L.W. eds. *Principles and Practice of Radiation Oncology. ch.15 -Hyperthermia* ; Perez C.A., B. Emami, G. Nussbaum, S. Sapareto, pp317-352.